

Transmitting high power rf acoustic radiation via fluid couplants into superstrates for microfluidics

Ryan P. Hodgson, Ming Tan, Leslie Yeo, and James Friend^{a)}

Micro/Nanophysics Laboratory, Monash University, Wellington Road, Clayton, Victoria 3800, Australia

(Received 10 August 2008; accepted 23 November 2008; published online 13 January 2009)

In this study, surface acoustic radiation is refracted from lithium niobate through a fluid coupling into a thin glass plate. We demonstrate and explain its propagation as an asymmetric Lamb wave along the glass plate with sufficient power to transport fluid droplets across the glass surface at 8 mm/s. Such technology enables the use of standard processing techniques to fabricate an inexpensive and disposable microfluidics device together with the power transmission capabilities of surface acoustic wave devices with an easily renewable coupling. © 2009 American Institute of Physics. [DOI: 10.1063/1.3049128]

A key challenge to providing effective lab-on-a-chip solutions is the ability to pump and manipulate small quantities of liquids in confined spaces. Most conceivable applications of lab-on-a-chip technology are constrained by surface tension, viscous losses, and the slow rate of diffusion. Given the importance ascribed to the area, many research groups have sought effective pumping, mixing, and manipulation technologies with only fair success.^{1,2} An interesting approach to solve these problems is the use of radio-frequency (rf) acoustics transmitted along a single-crystal piezoelectric material surface to impart kinetic energy into bulk objects,³ fluids, or particles^{4–6} within those fluids. Surface acoustic waves (SAWs)—especially Rayleigh waves—transmitted along such a surface provides up to several watts of power in a device commensurate with the scale desired for microfluidics, along with the mounting and packaging convenience absent from bulk wave (i.e., Love, bulk acoustic, or Langevin wave) devices. The interaction may be used to drive droplet rotation, particle collection, concentration and dispersion,^{5,6} transport,^{7,8} and even atomization^{9,10} through a combination of first-order effects from the compressional sound wave propagating in the fluid and second-order slow time-scale effects—better known as *acoustic streaming*.¹¹ Although these devices are effective, their integration into microfluidics with integrated circuit fabrication techniques optimized for silicon, glass, and polymer materials¹² such as polydimethylsiloxane is problematic: useful piezoelectric materials do not easily etch. Although microfluidics devices may be formed from sandwiching piezoelectric and such materials together¹³ to solve the fabrication problems, the issue of cost in doing so remains.

Here a different approach is adopted. The microfluidics device is presumed to be fabricated in glass or silicon by traditional, low-cost methods and subsequently driven by rf Rayleigh wave SAW via a fluid coupling layer from a piezoelectric single-crystal substrate set below the microfluidics device. An illustration of the concept is shown in Fig. 1. The advantage of separating the microfluidics device from the power source with a renewable coupling layer in simplifying the fabrication is evident, although the transmission efficiency and power available to the microfluidics device would

define the pragmatic feasibility of such a scheme. This study seeks to determine whether delivery of high power acoustic radiation through such a fluid coupling layer is effective for microfluidics applications, what the underlying physical mechanism is, and what the effect of different fluids and geometries in the behavior might be.

In Fig. 1 a single droplet of water—1, 3, or 5 μl —is placed upon a crown glass wafer (*superstrate*) 14 mm wide \times 10 mm long \times 150 μm thick, itself set atop a lithium niobate (LN) 127.68° y - x wafer with a fluid droplet sandwiched between the glass and LN materials. Both water and glycerin were used as coupling fluids to crudely assess the effect of viscosity on the coupling of the acoustic radiation into the superstrate, although only water was used for the droplet being actuated atop the glass superstrate. The glass superstrate was held at one side of the SAW device with a mounting that allowed precise control of the fluid couplant thickness.

Carelessly examining the propagation of the acoustic wave using simple wave theory suggests that this idea *will not work*. The propagation of acoustic radiation from a SAW device into a fluid layer above it occurs through diffraction at the *Rayleigh angle*, $\theta_R = \sin^{-1}(c_f/c_s) \approx 23^\circ$ for water and LN (see Fig. 1), where $c_f = 1482$ m/s and c_s are the wave speeds

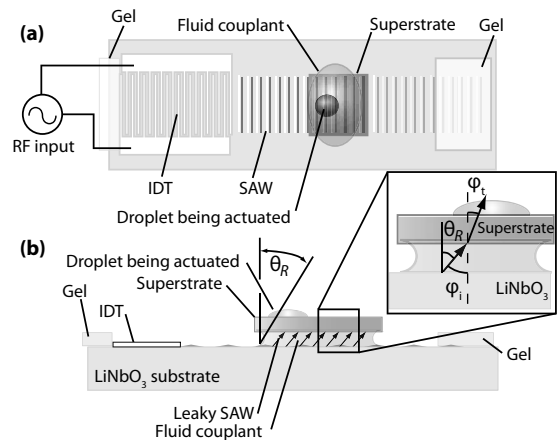


FIG. 1. Illustration of the fluid coupling of leaky SAW radiation into a superstrate containing the microfluidics device via a coupling fluid with (a) a top and (b) a side view. The vertical scale is exaggerated for clarity in the side view.

^{a)}Electronic mail: james.friend@eng.monash.edu.au. URL: <http://mnrl.monash.edu.au>.

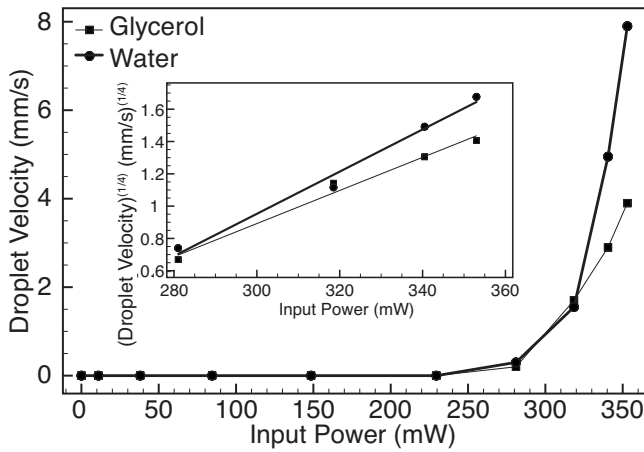


FIG. 2. Droplet velocity atop substrate vs input power; for those results with droplet motion, the (inset) one-fourth power of the droplet velocity appears to be linearly dependent on the input power. The coupling fluid is 28.6 μm thick and the droplet is 3 μl of water.

for the longitudinal wave in the fluid and the SAW, respectively. This is also the angle where the longitudinal sound waves approach the fluid-glass interface, $\phi_i \approx 23^\circ$. Naively using Snell's law, $\sin \phi_i = c_f \sin \phi_t / c_g = 1.34 > 1$, where c_g is the speed of a longitudinal sound wave in crown glass, $c_g = 5100$ m/s, indicates that the total reflection will occur off the interface.

However, it is indeed possible to form Lamb waves that propagate at far slower speeds¹⁴ in the thin glass layer from waves incident from the fluid. These waves are able to transmit sufficient power to the top of the superstrate to induce the droplet to move at up to 8 mm/s. Figure 2 indicates that the droplet will not move until a threshold power input—approximately 230 mW—is reached regardless of whether the couplant fluid is glycerin or water. Over this range of power, capillary waves appear on the surface of the droplet.⁹ For power levels where the droplet is forced to move, the fourth root of the droplet velocity is linearly dependent on the input power. The droplet velocity also increases with the size of the droplet as the thickness of the couplant layer increases from 7.14 to 28.6 μm , as shown in Fig. 3, while holding the input power constant at 350 mW. Although more rapid droplet motion is possible with this configuration, other phenomena also begin to appear as the power is raised above 350 mW, including droplet ejection and atomization.

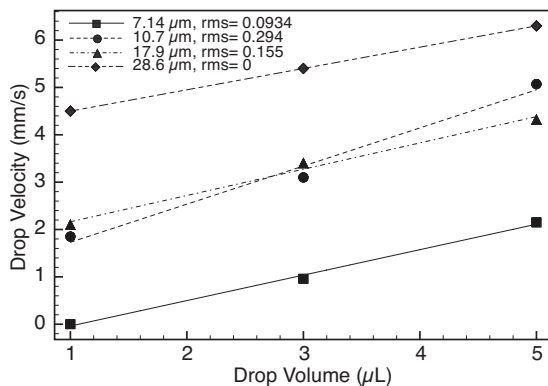


FIG. 3. Effect of couplant thickness and droplet size on the droplet velocity. The input power is held constant at 350 mW using water as the coupling fluid.

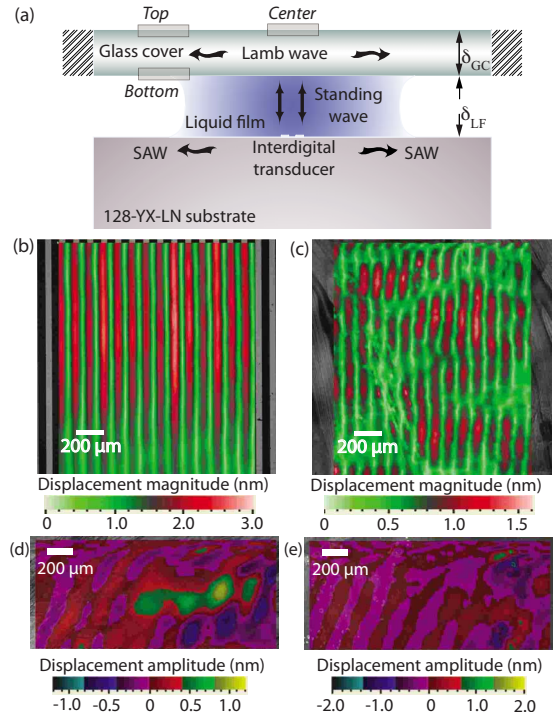


FIG. 4. (Color online) Laser Doppler vibrometer scan of the (a) superstrate system using a 28.57 μm thick water couplant layer. The magnitude of displacement transverse to the surface at 20 MHz (b) on the LN substrate shows the SAW at that same frequency; a similar wave appears (c) on the upper surface of the glass superstrate at center in (a), directly above the interdigital transducer; this wave appears to be an asymmetric, higher-order Lamb wave based on the similar wave pattern, amplitude, and phase measured on the (d) top and (e) bottom faces of the glass layer, respectively. The velocity amplitude is scaled differently in each layer for clarity.

The mechanism underlying these apparently conflicting results was examined using scanning laser Doppler vibrometry (LDV) (Polytec MSA-400, Waldbrunn, Germany), as shown in Fig. 4 and in more detail elsewhere.¹⁵ Here the LDV provides a map of the transverse displacement field at a

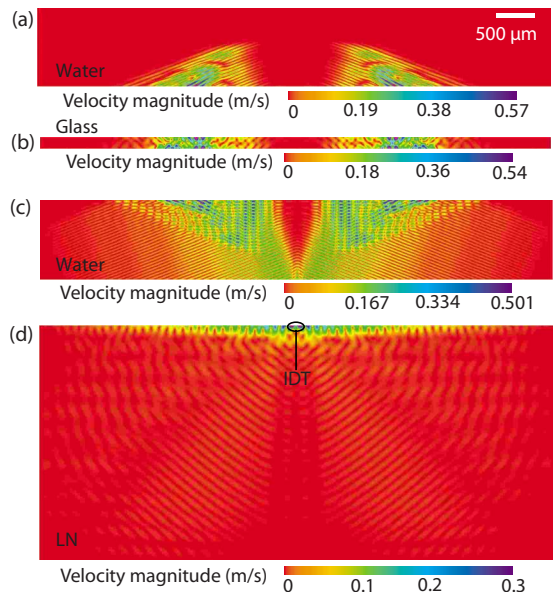


FIG. 5. (Color online) Side view of the bottom-up propagation of the acoustic radiation from (d) LN into (c) water, (b) glass, and then (a) water again, respectively, at 1250 ns after starting the SAW on the IDT atop the LN substrate.

surface at 20 MHz under narrowband operation; the top surfaces of the superstrate and the LN substrate below it were examined. The SAW appearing in the substrate has a wavelength of approximately 190 μm , as does the wave propagating along the upper surface of the glass. In this configuration, the wave in the superstrate is evidently a Lamb wave; the amplitude of the displacement along the top and bottom surfaces of the superstrate was similar (not shown) and traveled along the same direction away from the *center* indicated in Fig. 4. Furthermore, the amplitude of the wave along the top surface of the superstrate was approximately one-half the amplitude of the SAW in the LN, indicating reasonably good transmission of the acoustic radiation into the superstrate. Using a two-dimensional numerical analysis method detailed elsewhere,¹⁶ it is possible to examine the phenomena with more detail, as shown in Fig. 5. The radiation of leaky SAW in the water from the interdigital transducer (IDT) is clearly shown, and upon contact with the glass layer, the formation of a higher-order asymmetric Lamb wave that propagates along the glass in turn dissipates acoustic radiation into the fluid above it.

- ¹H. Stone, A. Stroock, and A. Ajdari, *Annu. Rev. Fluid Mech.* **36**, 381 (2004).
- ²D. Laser and J. Santiago, *J. Micromech. Microeng.* **14**, R35 (2004).
- ³K. Asai and M. Kurosawa, *IEEE Trans. Ultrason. Ferroelectr. Freq. Control* **52**, 1722 (2005).
- ⁴M. Tan, J. Friend, and L. Yeo, *Appl. Phys. Lett.* **91**, 224101 (2007).
- ⁵R. Shilton, M. K. Tan, L. Y. Yeo, and J. R. Friend, *J. Appl. Phys.* **104**, 014910 (2008).
- ⁶H. Li, J. Friend, and L. Yeo, *Phys. Rev. Lett.* **101**, 084502 (2008).
- ⁷M. Tan, J. Friend, and L. Yeo, *Lab Chip* **7**, 618 (2007).
- ⁸H. Li, J. R. Friend, and L. Y. Yeo, *Biomaterials* **9**, 647 (2007).
- ⁹A. Qi, L. Yeo, and J. Friend, *Phys. Fluids* **20**, 074103 (2008).
- ¹⁰J. Friend, L. Yeo, D. Arifin, and A. Mechler, *Nanotechnology* **19**, 145301 (2008).
- ¹¹W. L. Nyborg, in *Acoustic Streaming*, edited by W. P. Mason and R. N. Thurston (Academic, New York, 1965), Vol. 2B, Chap. 11, pp. 265–329.
- ¹²J. Anderson, D. Chiu, R. Jackman, O. Cherniavskaya, J. McDonald, H. Wu, S. Whitesides, and G. Whitesides, *Anal. Chem.* **72**, 3158 (2000).
- ¹³K. Sritharan, C. Strobl, M. Schneider, A. Wixforth, and Z. Guttenberg, *Appl. Phys. Lett.* **88**, 054102 (2006).
- ¹⁴R. White and S. Wenzel, *Appl. Phys. Lett.* **52**, 1653 (1988).
- ¹⁵See EPAPS Document No. E-APPLAB-93-072850 for an image describing the particle velocity distribution across the lithium niobate-water-glass-water system at (a–d) 750 ns, (e–h) 1250 ns, and (i–l) 1750 ns after starting the surface acoustic wave in the lithium niobate substrate. For more information on EPAPS, see <http://www.aip.org/pubservs/epaps.html>.
- ¹⁶L. Yeo and J. Friend, *Biomicrofluidics* **3**, 012002 (2009).